Numerical resolution of the heat accumulator in a Low Cost Cryogenic Propulsion (LCCP) system

Morales-Ruiz, S.⋆, Castro, J.⋆, Rigola, J.⋆, Pérez-Segarra, C. D.⋆, Oliva, A.⋆
⋆ *Centre Tecnològic de Transferència de Calor (CTTC); Universitat Politècnica de Catalunya (UPC); ETSEIAT, Colom 11, Terrassa (Barcelona), 08222, Spain*

Abstract

In this paper, a numerical study of a heat accumulator in the LCCP system has been carried out. The thermal and fluid-dynamic behaviour of the two-phase flow inside ducts working under cryogenic conditions as a propellant (LOX), coupled with the analysis of the phase change material (PCM) working as an accumulator element is presented. The numerical analysis is based on: i) a one-dimensional and transient integration of the governing equations for the fluid flow of propellant, and ii) a multi-dimensional and transient integration of the conservative equations in the volume occupied by the PCM, iii) the solid elements are modelled considering a multi-dimensional and transient treatment of the energy conservation equation. The numerical results of the heat accumulator analyzed are presented.

1. Introduction

In the European funded project: - In Space Propulsion-1 (ISP-1) -, fundamental knowledge about Low Cost Cryogenic Propulsion systems (LCCP) is being acquired. One of the components, the heat accumulator, stores thermal energy from the fuel cell that provides electrical energy to the whole system. This thermal energy is employed for the pressurisation of the propellant tanks. Two different types of heat accumulators are present in the LCCP system: the High Temperature Accumulator (HTA) and the Low Temperature Accumulator (LTA).

In a first stage, the study is focused on the LTA accumulator. The device consists of a set of tubes. Inside some of them the cryogenic flow of propellant (LOX) circulates. In the other tubes circulates a secondary flow (typically He or N2) that exchanges thermal energy with the fuel cell. Around the tubes there is a Phase Change Material (PCM-in this paper water-ice) that transfers the energy from the secondary fluid to the propellant. This unsteady process involves accumulation and disaccumulation of thermal energy in the PCM.

In this paper, a numerical study of the thermal and fluid-dynamic behaviour of the two-phase flow inside ducts working under cryogenic conditions, coupled with the analysis of the PCM accumulator is presented. The numerical analysis is based on: i) a one-dimensional and transient integration of the governing equations (conservation of mass, momentum and energy) for the fluid flow of propellant, and ii) a multi-dimensional and transient integration of the conservative equations in the region occupied by the PCM. The solid elements are modelled considering a multi-dimensional and transient treatment of the energy conservation equation.

The discretization of the governing equations has been developed by means of the finite volume technique using staggered meshes. The discretized mass, momentum and energy equations are solved using a pressure-based method SIMPLE-like [1]. This method has been applied to solve the thermal and fluid-dynamic behaviour of: the one-dimensional two-phase flow inside of the tube and the two-dimensional PCM confined in a cylinder domain.

The two-phase flow phenomena inside of the tube has been simulated considered the two-fluid model [2], which is an inter-penetrating model capable of defining the behaviour of the velocity, the pressure, the temperature and the distribution of each one of the phases, gas and liquid, separately. The fact that the two-fluid model takes into account unequal gas and liquid velocity in two-phase flow complex systems makes of this model an essential tool to evaluate the two-phase phenomenon under fast transient conditions. A group of parameters, used in the numerical model proposed, e.g. the heat transfer coefficient and the friction factor, are evaluated by means of empirical correlations, which have been obtained from the technical literature in the cryogenic field.

The phase change phenomenon of the PCM has been simulated by means of the numerical resolution of the conservative equations (mass, momentum and energy), using an enthalpy method [3]. The essential feature of this

method is that latent heat effects are isolated in a source term of the conservative equations. Also a technique to ensure that velocities predicted to be in a solid region actually take the value zero is required.

The wall tube temperature distribution is obtained after solving the discretized energy equation, where the heat conduction between tube and PCM, and the heat convection between tube and fluid flow have been considered as boundary conditions.

The global numerical algorithm takes into account, in a coupled manner, the thermal and fluid dynamical behaviour of the different elements of the system: i) the two-phase fluid flow of propellant inside the primary tubes (evaporation phenomena); ii) the PCM phase change solid-liquid; and iii) the heat conduction through the solid elements (the tubes).

Different numerical aspects have been evaluated with the aim of verifying the quality of the numerical solutions. Thus, convergence error, discretization error and numerical schemes have been analyzed. Numerical results of the whole system are shown, where the temperature distribution, pressure, void fraction and velocities of the fluid flow, together with the wall tube and PCM temperature are presented.

2. Mathematical Model

The mathematical model proposed to solve the two-phase flow inside a tube, the PCM and the solid element is detail in next section:

2.1 Fluid flow

Mathematical formulation is based on the application of the conservative equations on each phase, liquid and gas. Then, six-equations are obtained: continuity, momentum and energy for each phase [2]. The assumed hypotheses are: one-dimensional flow, constant cross section, and negligible axial heat conduction in fluid. The governing equations for the two phases are:

$$\frac{\partial}{\partial t}(\alpha_l \rho_l) + \frac{\partial}{\partial z}(\alpha_l \rho_l v_l) = -\Gamma_g \tag{1}$$

$$\frac{\partial}{\partial t}(\alpha_g \rho_g) + \frac{\partial}{\partial z}(\alpha_g \rho_g v_g) = \Gamma_g \tag{2}$$

where α_g and α_l are the gas and liquid void fraction, v_l and v_g are the liquid and gas velocities, and Γ_g is the gas mass transfer rate per unit volume.

The momentum equations for each phase is expressed as:

$$\frac{\partial}{\partial t}(\alpha_l \rho_l v_l) + \frac{\partial}{\partial z}(\alpha_l \rho_l {v_l}^2) = -\alpha_l \frac{\partial p}{\partial z} - \frac{P_{wl}\tau_{wl}}{S} - \alpha_l \rho_l g sin\theta - \frac{P_i \tau_{il}}{S} - \Gamma_g v_{il} \tag{3}$$

$$\frac{\partial}{\partial t}(\alpha_g \rho_g v_g) + \frac{\partial}{\partial z}(\alpha_g \rho_g {v_g}^2) = -\alpha_g \frac{\partial p}{\partial z} - \frac{P_{wg}\tau_{wg}}{S} - \alpha_g \rho_g g sin\theta - \frac{P_i \tau_{ig}}{S} + \Gamma_g v_{ig} \tag{4}$$

where p is the total pressure, θ is the inclination angle of the pipe, τ_{wg} and τ_{wl} are the shear stresses acting on the gas and liquid phase at the wall, respectively, and τ_i is the shear stress between phases at the interface. The wall perimeter in contact with the liquid and gas is denoted by P_{wl} and P_{wg}, while S is the flux cross section area.

The energy equations expressed in terms of enthalpy are:

$$\frac{\partial}{\partial t}(\alpha_l \rho_l h_l) + \frac{\partial}{\partial z}(\alpha_l \rho_l v_l h_l) = -\frac{\dot{q}_{wl} P_{wl}}{S} + \alpha_l \frac{\partial p}{\partial t} - \Gamma_g h_{il} + \frac{\dot{q}_{il} P_{il}}{S} \tag{5}$$

$$\frac{\partial}{\partial t}(\alpha_g \rho_g h_g) + \frac{\partial}{\partial z}(\alpha_g \rho_g v_g h_g) = -\frac{\dot{q}_{wg} P_{wg}}{S} + \alpha_g \frac{\partial p}{\partial t} + \Gamma_g h_{ig} + \frac{\dot{q}_{ig} P_{ig}}{S} \tag{6}$$

where $\dot{q}_{il}$ and $\dot{q}_{ig}$ are the heat transfer exchanged at the interface, while $\dot{q}_{wl}$ and $\dot{q}_{wg}$ are the heat transfered from the wall to the liquid and gas phase, respectively. These quantities are evaluated by means of empirical expressions.

2.2 Phase change material (PCM)

Mathematical formulation of the PCM is based on the conservative equations of mass, momentum and energy. An enthalpy method for convection diffusion phase change is used [3]. The essential feature of this method is that latent heat effects are isolated in a source term and a technique is required to ensure that velocities predicted to be in a solid region actually take the value zero. The governing equations for the PCM are:

$$\frac{\partial u}{\partial z} + \frac{1}{r}\frac{\partial (rv)}{\partial r} = 0 \tag{7}$$

$$\rho\left[\frac{\partial u}{\partial t} + \frac{\partial u^2}{\partial z} + \frac{1}{r}\frac{\partial (ruv)}{\partial r}\right] = -\frac{\partial p}{\partial z} + \mu\left[\frac{1}{r}\frac{\partial}{\partial r}\left(r\frac{\partial u}{\partial r}\right) + \frac{\partial^2 u}{\partial z^2}\right] + \rho g_z \beta (T - T_{ref}) + Au \tag{8}$$

$$\rho\left[\frac{\partial v}{\partial t} + \frac{\partial (uv)}{\partial z} + \frac{1}{r}\frac{\partial (rv^2)}{\partial r}\right] = -\frac{\partial p}{\partial r} + \mu\left[\frac{1}{r}\frac{\partial}{\partial r}\left(r\frac{\partial v}{\partial r}\right) + \frac{\partial^2 v}{\partial z^2} - \frac{v}{r^2}\right] + \rho g_r \beta (T - T_{ref}) + Av \tag{9}$$

$$\frac{\partial T}{\partial t} + \frac{\partial (uT)}{\partial z} + \frac{1}{r}\frac{\partial (rvT)}{\partial r} = \frac{\lambda}{\rho c_p}\left[\frac{1}{r}\frac{\partial}{\partial r}\left(r\frac{\partial T}{\partial r}\right) + \frac{\partial^2 T}{\partial z^2}\right] - \frac{H}{c_p}\frac{\partial f_l}{\partial t} \tag{10}$$

where u is the axial velocity component, v is the radial velocity component, T is the PCM temperature, T_{ref} is a reference temperature used to evaluate the Boussinesq term, f_l is the liquid fraction, A is a parameter, which defines the velocity value as zero when solid phase is present, it is evaluated as $A = -C(1 - f_l)^2/(f_l^3 + b)$ using $C = 10^9$ y $b = 10^{-6}$, H is the latent heat of phase change.

2.3 Solid elements

The solid element (wall tube) is evaluated by means of the energy equation. A two-dimensional and transient integration of this equation allow obtain the temperature distribution of the wall tube.

$$\rho c_p \frac{\partial T}{\partial t} = \frac{\partial}{\partial z}\left(\lambda\frac{\partial T}{\partial z}\right) + \frac{1}{r}\frac{\partial}{\partial r}\left(\lambda\frac{\partial T}{\partial r}\right) \tag{11}$$

An schematic representation of the heat accumulator in a LCCP system is depicted in Figure 1, together with a typical discretization used in the whole system (the fluid flow, the wall tube, and the PCM).

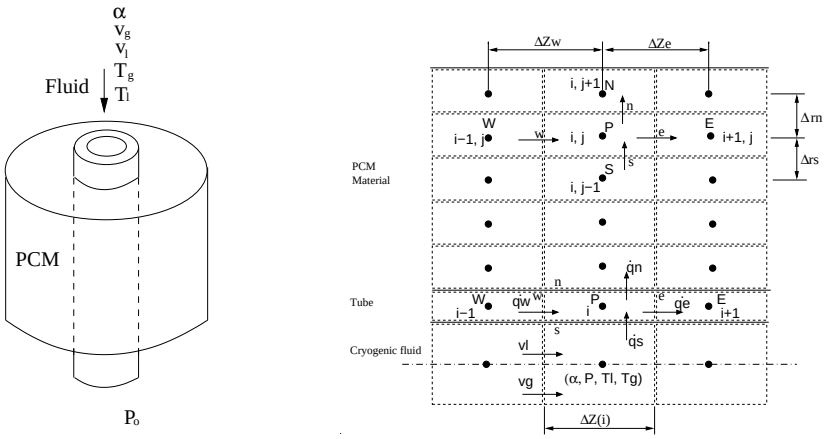

Figure 1: Schematic representation of the PCM heat accumulator, and the mesh used in the discretization

3. Empirical correlations

Definition of the regime is necessary to choose the correct empirical correlation. Factors such as frictional coefficients, heat transfer coefficients and interfacial area are obtained by means of the empirical correlations. Different regimes can be present into the inner tubes. Geometry, position, velocity and heat condition are some parameter that affect the kind of regimes present. A simplified scheme is used to evaluate the regime as function of the void fraction, velocity and position. Bubbly, slug, annular, dispersed flow and combination of them can occur in horizontal or vertical tubes.

Heat transfer from interface to gas phase q_{ig} and to liquid phase q_{il} are evaluated with heat transfer coefficients at interface. In the same form, heat transfer from wall to gas phase q_{wg} and to liquid phase q_{wl} are calculated with heat transfer coefficient assumed that only one phase is present in the flux.

$$\left[\frac{\dot{q}_{il}P_{il}}{S}\right] = h_{TC,il}(T_{sat} - T_l) \tag{12}$$

$$\left[\frac{\dot{q}_{ig}P_{ig}}{S}\right] = h_{TC,ig}(T_{sat} - T_g) \tag{13}$$

$$\left[\frac{\dot{q}_{wl}P_{wl}}{S}\right] = h_{TC,wl}(T_w - T_l) \tag{14}$$

$$\left[\frac{\dot{q}_{wg}P_{wg}}{S}\right] = h_{TC,wg}(T_w - T_g) \tag{15}$$

The group of heat transfer coefficients values have been evaluated by means of empirical correlations, which depend on the flow regime. Therefore, two group of expressions are written in function of two different flow regimes: inverted annular flow and dispersed flow. Both are present in the case analyzed in results.

Inverted annular flow:

$$h_{TC,ig} = \begin{cases} \frac{\lambda_g Nu_i}{2\delta} & \text{for } (\delta << R) \\ \frac{\lambda_g}{2\delta}(0.023{Re_i}^{0.8}{Pr_g}^{0.33}) & \text{otherwise} \end{cases} \tag{16}$$

$$h_{TC,wg} = \begin{cases} \frac{\lambda_g Nu_w}{2\delta} & \text{for } (\delta << R) \\ \frac{\lambda_g}{2\delta}(0.023{Re_w}^{0.8}{Pr_g}^{0.33}) & \text{otherwise} \end{cases} \tag{17}$$

where δ is the vapour layer thickness, $\delta = R(1 - (1 - \alpha)^{0.5})$, R is the tube radius, the Nusselt number at the interface, Nu_i, and at the wall, Nu_w, are assumed as 5.385 for laminar flow and 27.8 for turbulent flow [4], Reynolds number at interface, $Re_i = \rho g|v_g - v_l|2\delta/\mu_g$, and at the wall $Re_w = \rho g v_g 2\delta/\mu_g$.

Dispersed flow:

$$_{TC,ig} = \frac{\lambda_g}{d}(2.0 + 0.74{Re_d}^{0.5}{Pr_g}^{0.33}) \tag{18}$$

$$h_{TC,wg} = 0.023\frac{\lambda_g}{D}{Re_g}^{0.8}{Pr_g}^{0.33}) \tag{19}$$

$$h_{TC,wl} = \left[\frac{10{\lambda_g}^3{t_R}^3\rho_g{h_{lg}}^o{\dot{m}_d}^5}{{d^5\rho_l}^4\mu_g(1-\alpha_g)(T_w - T_s)}\right]^{1/4} \tag{20}$$

$$d = 0.00796\frac{\sigma}{\rho_g(\alpha v_g)^2}{Re_g}^{2/3}(\rho_g/\rho_l)^{-1/3}(\mu_g/\mu_l)^{2/3} \tag{21}$$

where d is the droplet diameter, Re_d is the droplet Reynolds number, $Re_d = \rho_g|v_g - v_l|d/\mu_g$, t_R is the droplet resident time, $t_R = \pi(\rho l d^3 d^3 16\sigma)^{0.5}$, the modified latent heat is evaluated as $h^o_{lg} = h_{lg} + c_p(T_g - T_s)$, and $\dot{m}_d$ is the deposition rate, $\dot{m}_d = 0.22(\mu_l/D)Re_l 0.74(\mu_g/\mu_l)(1-\alpha_g)\rho_l$ [5].

The verification of the empirical correlations has been carried out by means of the numerical and experimental comparison of the heat transfer coefficient. The comparison between the experimental data obtained from literature [6] and the numerical results obtained with the expressions presented above are presented in Table 1.

Table 1: Numerical and experimental comparison of the heat transfer coefficient (wall-gas)

q_w (kW/m^2)	T_w (K)	T_g (K)	$h_{TC,exp}$ (W/m^2K)	$h_{TC,num}$ (W/m^2K)	$Error$ $(\%)$
8000	673	470	39.40	37.68	4.36
7000	753	575	39.32	40.69	3.48
5500	843	723	45.80	41.70	8.95
4500	883	773	40.90	41.63	1.78

Mass transfer rate per unit of volume Γ_g is the sum of the mass transfer at the interface Γ_{ig} by increment of energy of the one phase and the mass transfer from the wall to interface Γ_w by action of the external heat transfer. This value is obtained by means of the energy balances at the interface and at the wall.

$$\Gamma_w = -\frac{\dot{q}_{wg}P_{wg} + \dot{q}_{wl}P_{wl}}{S(h_g - h_l)_{sat}} \tag{22}$$

$$\Gamma_i g = -\frac{\dot{q}_{ig}P_{ig} + \dot{q}_{il}P_{il}}{S(h_g - h_l)_{sat}} \tag{23}$$

$$\Gamma_g = \Gamma_w + \Gamma_{ig} \tag{24}$$

In these expression $(h_g - h_l)_{sat}$ is a difference of enthalpies at saturation condition.

4. Numerical Resolution

The global numerical algorithm to solve the whole system takes into account, in coupled manner, the thermal and fluid dynamical behaviour of the different elements: i) the two-phase flow inside the tube, ii) the PCM, and iii) the wall tube.

The two-phase flow is simulated by means of the numerical resolution of the equations (1) to (6) as a first step. The discretized equations have been obtained ordering these equations in a generic one-dimensional form $a_P\phi_P = a_E\phi_E + a_W\phi_W + b_P$. The set of algebraic equations is solved using the three diagonal matrix algorithm TDMA. The coupling between momentum and continuity is solved by means of the semi-implicit pressure based method SIMPLEC [1]. One way to solve the strong coupling between two momentum and two continuity equations, together with the effect of the interface drag and mass transfer is written explicitly the interfacial terms in continuity, momentum and energy equation and solve the set of equations to obtain a pseudo-solution which resolves the interphase coupling [7]. Taking into account this aspect, the steps to evaluate the fluid consists of solving implicitly velocities v_k, using guess pressure $p*$ and density $\rho*$ fields. After that, solve the pressure correction equation to obtain the pressure correction value p' and correct with it the velocities $v_k = v_k * + v_k'$, pressure $p = p * + p'$ and densities $\rho_k = \rho_k p'/\varphi p*$. Next, the void fraction is solved, together with the energy equations in function of enthalpy, h_k, using the updated values of pressure and velocities, and the guess wall temperature distribution $T_w{}^*$.

The PCM is simulated by means of the numerical resolution of the equations (7) to (10) as a second step. These equations have been discretized and organized in a generic two-dimensional form $a_P\phi_P = a_E\phi_E + a_W\phi_W + a_N\phi_N + a_S\phi_S + b_P$. The set of algebraic equations resultant is solved using the SIMPLEC method. The numerical results of the axial and radial velocity, pressure, temperature and liquid fraction (u, v, P, T and f_l) of the PCM have been obtained using the guess wall temperature $T_w{}^*$ as a boundary condition. After the fluid flow and the PCM are evaluated, a new wall temperature should be calculated.

The wall tube temperature is obtained from the numerical resolution of the equation (11), which has been discretized and organized in a generic two-dimensional form $a_P\phi_P = a_E\phi_E + a_W\phi_W + a_N\phi_N + a_S\phi_S + b_P$. This algebraic equation is solved by means of the SOR algorithm, using the PCM temperature distribution and the convective heat transferred from the fluid flow as boundary conditions, both evaluated before (first and second steps). An new wall temperature T_w is obtained, this value should be updated into the fluid flow and the PCM resolution algorithm.

Once, the fluid flow, the PCM and the wall tube have been solved, return to the first step and an iterative process should be made until the convergence criteria is reached in all elements. The convergence of the whole system is based on the maximum difference between the different local variables at the previous iteration ϕ^* and at the actual one ϕ, i.e. $(max|\phi - \phi^*|/\phi) < \delta$, where δ is the convergence criteria. The process run step-by-step in the time direction until a steady-state or some specific period of time is reached.

5. Results

5.1 Sedimentation

This case is a simplified gravity-induced phase separation problem [8]. The most important characteristic of the sedimentation problem is the transition from two-phase flow to single-phase flow. The case is also useful to test the stability of the numerical resolution method. The sedimentation problem consists of a vertical pipe of length $7.5m$ where, gravity is the only source term considered. Initially, at time t=0.0s, the pipe is filled with a uniform mixture of liquid and gas, at pressure p = $10^5 Pa$ and a gas void fraction of 0.5. The pipe is closed at both ends. Velocities at the top and the bottom boundaries are considered to be zero. The gravity field provides a separation of the phases for t> 0. The solution at t = ∞ is composed of a pure gas at rest at the top side, and a liquid at rest at the bottom side of the pipe.

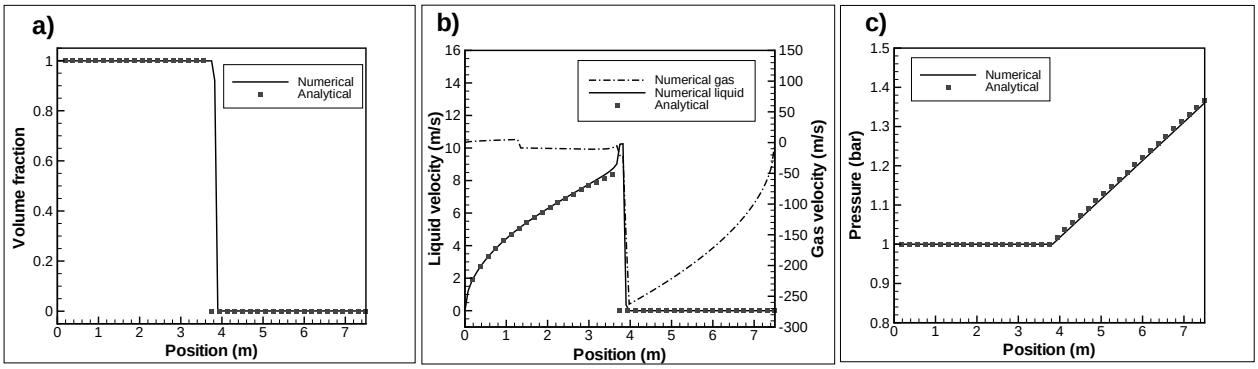

Figure 2: Sedimentation case: comparison between numerical results and analytical solution at 1.0s [9]

The results have been obtained using a mesh of 40 CVs, a time step of $\Delta t = 10^{-3} s$, and assuming the liquid and gas density of $1000 kg/m^3$ and $1.0 kg/m^3$, respectively. Numerical results have been compared with an analytical solution obtained from technical literature [9], which proposed a set of mathematical expressions for the evaluation of void fraction, liquid velocity and pressure. The comparison between analytical solution and numerical results obtained with the model proposed in this paper at time instant 1.0s are depicted in Figure 2. Reasonable good agreement can be observed.

5.2 A heat accumulator in LCCP system

This is an illustrative case, where the liquid oxygen flow is always exchanging heat along the tube length, while the tube is exchanging heat outside with the PCM. The thermal and fluid dynamic behaviour of the fluid and the PCM are shown. A schematic representation is depicted in Figure 1.

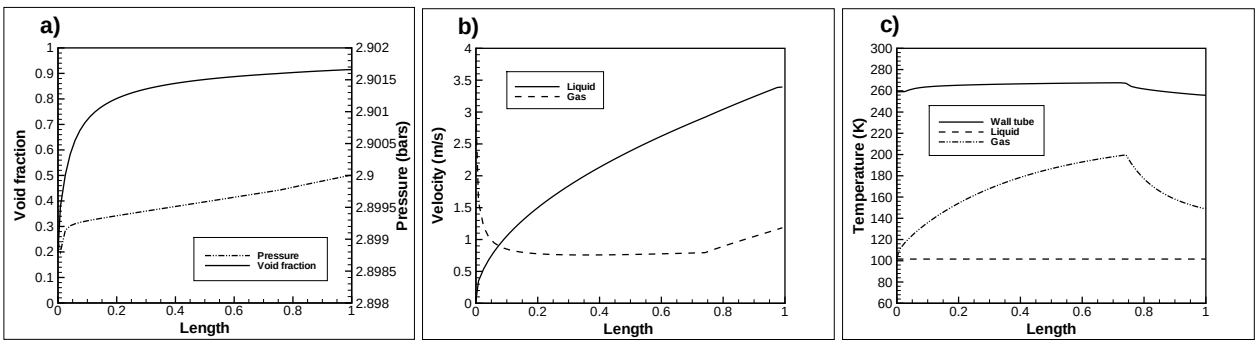

Figure 3: Numerical results of the two-phase flow. a) pressure and void fraction; b) velocities; and c) temperatures.

The fluid flow boundary conditions are liquid velocity $0.04 m/s$, gas velocity $3.0 m/s$, void fraction 0.2, saturation temperature of liquid and gas $101 K$ at the inlet and pressure 2.9 bars at the outlet. The wall tube is adiabatic at the top

and at the bottom extremes. The initial condition of the wall tube temperature is $273K$ along the length, while the PCM temperature is $273K$ assuming solid phase.

A mesh size of 60 control volume, CV, has been used in the fluid flow resolution, while the PCM has been solved with a mesh size of 600 CVs. A time step of $\Delta t = 10^{-4}s$ has been used to find a transient solution at time $10s$.

The void fraction of the two-phase flow inside the tube is depicted in Figure 3a, where the evolution from 0.2 to 0.9 of the gas void fraction along the tube is shown. The oxygen flow was not evaporated totally inside the tube in the case studied. This case presents two different flow regimes: the inverted annular flow in the first part and the dispersed flow at the end, following the regimes map criteria obtained from the literature. Along the dispersed regime an inefficient heat transfer mechanism appears. Therefore, the energy supplied from the wall is not enough to evaporate the liquid droplets, which are flowing into the gas flow. This aspect is being studied in our group.

The pressure behaviour of the fluid along the tube is shown in Figure 3a. Although, the pressure value at the inlet is less than the value at the outlet as a consequence of the gravity, the pressure drop along the length is small. The liquid and gas velocities evolution are depicted in the Figure 3b. The liquid velocity value increases from the inlet to the outlet of the tube, whiles the gas velocity value decreases at the initial part of the length during the inverted annular flow regime, and changes its behaviour at point 0.75, when the dispersed flow regime appears in the flow.

The wall, gas and liquid temperatures are shown in Figure 3c, where the wall and liquid temperatures have not presented significant changes along the length, while the gas temperature suffers a change at point 0.75 as a consequence of the flow regime change from inverted annular to dispersed flow regime. A possible reason to explain the gas temperature decrease is that the interfacial area suffers an increase, due to the liquid droplets appearance. This fact produces that part of the energy used to heat the gas phase during the inverted annular flow will be required to evaporate the liquid droplets.

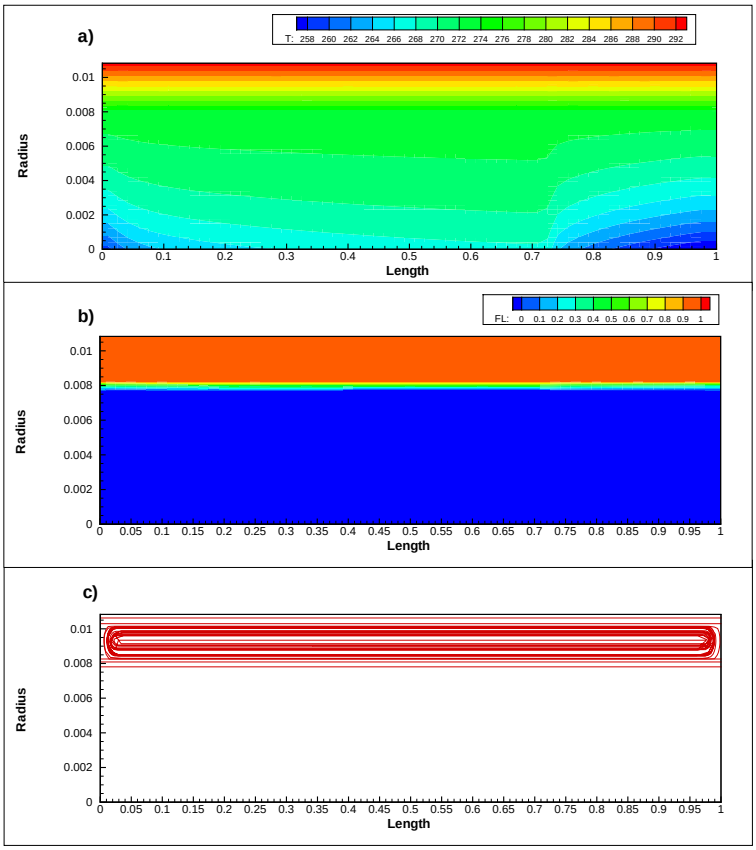

Figure 4: Numerical results of the PCM: a) temperature distribution; b) liquid fraction; and c) streamtraces.

The PCM temperature distribution is shown in Figure 4a, in which the two different surfaces are well defined. The temperature distribution decreases on the bottom surface in contact with the wall tube, as a consequence of the heat transferred from the PCM to the wall tube, whiles the temperature on the top surface increases its value as a

consequence of the heat transferred from the environment to the PCM. This case has been simulated assuming an environment temperature of $293K$, this value is used to fix the boundary condition outside of the PCM.

The solid-liquid distribution of the PCM into the cylinder domain is illustrated in Figure 4b. This is the evolution of the PCM liquid fraction, f_l, at time $10s$ as a consequence of the PCM melting by the heat exchanged with the environment. The numerical results of the PCM shows how a fifth part of the volume occupied by the PCM has changed from solid to liquid.

The streamtraces of the PCM are depicted in Figure 4c. The movement of the PCM liquid-phase into the cylinder domain follow the red lines, while the velocity in the solid region is zero. Complying with the requirement of the enthalpy method, which ensures that velocities predicted to be in a solid region take the value zero.

6. Conclusions

This paper has shown a numerical method to solve the two-phase flow inside pipes, together with the phase change, solid-liquid, of the PCM and the wall tube. The mathematical formulation of the fluid flow is based on the two-fluid model, while the enthalpy formulation is applied to evaluate the PCM. The governing equations discretization has been carried out by means of the control volume technique. A numerical algorithm capable to solve the couple between velocities and pressure in the fluid flow, and the influence of the PCM and wall tube has been implemented, together with a group of empirical correlations. These correlations have been used to evaluate the different parameters required in the set of algebraic equations that define the two-phase flow behaviour. After that, verification of the code has been presented with a well-known benchmark case, the Sedimentation, in which the influence of the gravity force in the numerical resolution has been analyzed. At the end, the thermal and fluid dynamic behaviour of a heat accumulator LCCP system has been studied, which shows the potential use of the model developed in this paper to describe the different elements of the whole system. The heat accumulator case, which is working under cryogenic conditions, has been used to test the stability of the numerical resolution method presented in this paper. A fast transient evaluation of the whole system has been carried out, where the evolution of the phase change of the PCM and the boiling process of the fluid flow have been presented.

Acknowledgements

This work has been performed by the financial support of the European Commission, contract № 218849.

References

[1] S. V. Patankar. *Numerical Heat Transfer and Fluid Flow*. Hemisphere Publishing Corporation, 1980.

[2] M. Ishii and T. Hibiki. *Thermo-fluid dynamics of two-phase flows.* Springer, 2006.

[3] V. R. Voller, M. Cross, and N. Markatos. An enthalpy method for convection/diffusion phase change. *International Journal for Numerical Methods in Engineering*, 24(1):271–284, 1987.

[4] K. Yuan, Y. Ji, and J. N. Chung. Numerical modeling of cryogenic chilldown process in terrestrial gravity and microgravity. *International Journal of Heat and Fluid Flow*, 30:44–53, 2009.

[5] Y. Gou and K. Mishima. A Non-equilibrium mechanistic heat transfer model for post-dryout dispersed flow regime. *Exp. Thermal and Fluid Science*, 26:861–869, 2002.

[6] M. M. Shah and M. A. Siddiqui. A General Correlation for Heat Transfer during dispersed-flow film boiling in tubes. *Heat Transfer Engineering*, 21:18–32, 2000.

[7] M. Darwish and F. Moukalled. A unified formulation of the segregated class of algorithms for multiphase flow at all speeds. *Numerical Heat Transfer, Part B*, 40:99–137, 2001.

[8] F. Coquel, K. El Amine, E. Godlewski, B. Perthame, and P. Rascle. A numerical method using upwind schemes for the resolution of two-phase flows. *Journal of Computational Physics*, 136:272–288, 1997.

[9] S. Evje and T. Flatten. Hybrid flux-splitting schemes for a common two-phase flow model. *Journal of Computational Physics*, 192:175–210, 2003.